SLAC-PUB-2827
October 1981
(T/E)

νN, μN INTERACTIONS: STRUCTURE FUNCTIONS, HIGHER TWIST*

C. Matteuzzi
Stanford Linear Accelerator Center
Stanford, California 94305

INTRODUCTION

Data on deep inelastic scattering of leptons by nucleons and nuclei have been accumulated for several years. Results exist from several experiments with electron, muon, neutrino beams. In this talk I shall review the most recent experiments (listed in Table I) which measured nucleon structure functions with ν and μ beams. In particular, I will summarize the results on $R = \sigma_L/\sigma_T$ measurement, on $F_2(x, Q^2)$ and $xF_3(x, Q^2)$, and their interpretation in terms of QCD, including both gluon radiation and higher twist phenomena.

Invited talk presented at the
Annual Meeting of the Division of Particle and Fields of the APS,
Santa Cruz, California
September 9-11, 1981

*Work supported by the Department of Energy Contract, DE-AC03-76SF00515.

Recent Experiments

Muon experiments listed in Table I have very good statistics and consequently the systematics dominate in the the treatment of the data. The experiment performed with the Multi Muon Spectrometer at Fermilab by the Berkeley-FNAL-Princeton collaboration provides results on the charm component of the structure functions and its role in scale non invariance. It will be discussed in the next talk by M. Strovink.[4]

Table I. Most recent experiments providing results on nucleon structure functions.

Muon Experiments				
Ref	Expt	Target	E_{Beam} (Gev)	# events
1	BCDMS (NA_4 CERN)	Carbon	120	10^5
			200	10^5
2	EMC (NA_2 CERN)	Iron	120	5.4×10^5
			250	2.0×10^5
			280	7.0×10^4
		Hydrogen	120	10^5
			280	1.4×10^5
3	PBF (MMS, FNAL)	Iron	209	8.0×10^4 $\mu\mu$

Neutrino Experiments				
Ref	Expt	Target	Beam	# events
5	BEBC (ABPPST)	D_2	WBB ν	1.5×10^3
			$\bar{\nu}$	6.0×10^3
6	CDHS	Fe	NBB ν	10^5
			$\bar{\nu}$	2.5×10^4
			WBB ν	6.0×10^4
			$\bar{\nu}$	1.5×10^3
7	CFRR	Fe	NBB ν	5.8×10^4
			$\bar{\nu}$	1.7×10^4
8	CHARM	Marble	NBB ν	6.3×10^3
			$\bar{\nu}$	6.3×10^3
9	GGM	C_3H_8	WBB ν	3.0×10^3
			$\bar{\nu}$	3.8×10^3

Except for the CDHS and the CFRR experiments, neutrino data generally have poor statistics. The nucleon structure functions $F_i(x, Q^2)$ are now known with good accuracy over a range of $Q^2 \approx 1 - 200$ GeV^2.

Structure Functions

Lepton hadron scattering is sketched in Fig. 1. The relevant kinematic quantitites are:

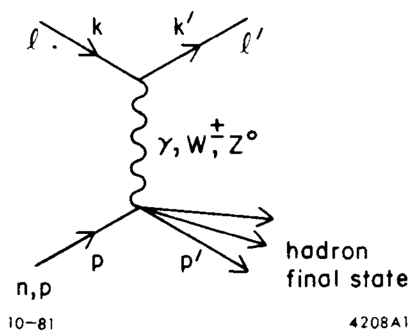

Fig. 1. Diagram for lepton-hadron scattering.

$$Q^2 = 4EE_{\ell'} \sin^2 \theta/2 \quad ,$$

$$\nu = p.(k - k')/m \quad ,$$

$$x = Q^2/2m\nu \quad ,$$

$$y = m\nu/p.k \tag{1}$$

where m is the nucleon mass and E the incident lepton energy.

The cross section for the process is

$$\frac{d^2\sigma}{dxdy} = \frac{4\alpha^2\pi Em}{Q^2}\left\{\left[1 + (1-y)^2\right] F_2(x,Q^2) - y^2R.2xF_1(x,Q^2)\right\} \tag{2}$$

when ℓ is charged and

$$\frac{d^2\sigma}{dxdy} = \frac{G^2Em}{\pi\left(1 + \frac{Q^2}{M_W^2}\right)}\left\{\left[1 + (1-y)^2\right] F_2(x,Q^2) - y^2R.2xF_1(x,Q^2) \overset{+}{(-)} (2y - y^2)xF_3(x,Q^2)\right\} \tag{3}$$

when ℓ is ν ($\bar{\nu}$).

R measures the contribution of longitudinally polarized γ or $W^{\pm}$ and

$$R = \frac{\left[F_2\left(1 - \frac{4m^2x^2}{Q^2}\right) - 2xF_1\right]}{2xF_1} = \sigma_L/\sigma_T \quad . \tag{4}$$

To reduce the number of independent F_i, one assumes charge symmetry and scattering on isoscalar targets. Furthermore, unless R is measured in a given experiment, a value for it must be assumed before F_2 can be extracted. In the language of the simple Quark Parton Model (QPM), F_2 measures the $q + \bar{q}$ momentum distribution in the nucleon, xF_3 the valence quark momentum distribution, and R is 0, if m^2/Q^2 terms are neglected, because the scattering on spin 1/2 objects implies $2xF_1 = F_2$.

Corrections

Each data set has to be corrected for several effects before structure functions are calculated:

1. Non-isoscalar target correction.
2. Radiative corrections. Usually only radiation from the incoming and outgoing μ in μ scattering and the outgoing μ in ν scattering is considered. Radiative effects underestimate the true σ at large x and overestimate it at low x. The corrections are large (and Q^2 dependent) at the extreme values of x.
3. The weak electromagnetic interference due to Z^o exchange in μ scattering ($\sim$ -5% at Q^2 = 200 GeV^2 for μ^+). This correction depends on Q^2 but does not change very much with x.
4. Fermi motion in a nuclear target. This effect becomes important only at x > .8. It is typically +4% at x < .25, -15% at $x \approx .65$.
5. Correction for the strange sea in ν scattering. This effect is large at small x, and it could reach 20%. The strange sea has been determined experimentally from charm production by ν's[19] and $\bar{u} = \bar{d} = 2\bar{s}$ rather than SU(3) symmetric.
6. Acceptance and calibration of the detector.

All these corrections are sources of systematic errors, together with the uncertainty in the luminosity.

Measurement of R

In the QPM, R = 0. There are different effects which can make $R \neq 0$: a) the finite mass of the target, b) p_t with respect to the γ or W direction due to primordial transverse momentum or gluon emission or other dynamical effects.

To measure $R(x, Q^2)$ is undeniably a difficult task for, as indicated in Eqs. (2) and (3), it requires separating the term which varies as y^2 from the dominant $[1 + (1-y)^2]$ dependence. Since $y \propto 1/E$ at fixed x and Q^2, in μ experiments, this requires separate runs at different incident energies. In ν experiments, R can be measured from the sum $d\sigma^{\nu} + d\sigma^{\bar{\nu}}$. A summary of experimental results is given in Table II.

Table II. Results on $< R > = \sigma_L/\sigma_T$.

Exp	x range	Q^2 range (GeV^2)	< R >	Ref.	
GGM	0 - 1.	<1	.32 ± .15	10	NEUTRINO
BEBC	0 - .8	14	.11 ± .14	11	NEUTRINO
FMII	0 - 1.	4	-.12 ± .16	12	NEUTRINO
CDHS	0 - .6	25	.1 ± .07	6	NEUTRINO
HPWF	0 - .8	25	.18 ± .07	13	NEUTRINO
SLAC-MIT	.1 - .8	1 - 16	.14 ± .06	14	ELEC-TRON
SLAC	.1 - .8	1 - 16	.30 ± .1	15	ELEC-TRON
CHIO 1977	.001 - 1.	1 - 5	.05 ± .33	16	MUON
CHIO 1979	.003 - .1	.4 - 30	.52 ± .35	17	MUON
EMC	.03 - .65	3 - 170	μp .03 ± .10 μFe -.13 ± .19	18	MUON

One has to be careful in comparing the values in Table II, for the ranges of x and Q^2 are different. The errors on R are large. While not a big influence on the absolute value of F_2, poor knowledge of R leads to an appreciable uncertainty in the measurement of the Q^2 dependence of F_2.

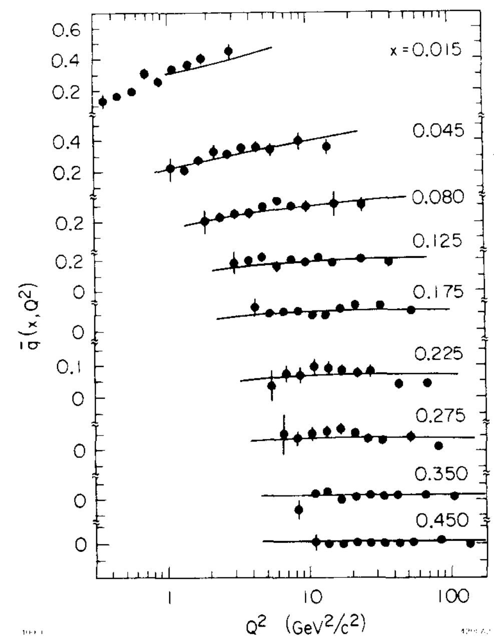

Fig. 2. $\bar{q}(x, Q^2)$ measured by the CDHS collaboration with $\bar{\nu}$ interactions.

Measurement of $\bar{q}$, F_2, xF_3

From the high y region of 175,000 $\bar{\nu}$ interactions, the CDHS collaboration has measured[19] the antiquark distribution $\bar{q}(x, Q^2)$ assuming R = .1 (Fig. 2). Two important features are noted: at small x, $\bar{q}$ rises with increasing Q^2, and there are no light antiquarks above x = 0.4. This provides an important constraint on the gluon distribution.

Data on $F_2(x, Q^2)$ exist over a quite extended range of Q^2. Figure 3 shows EMC and BCDMS muon data, which agree nicely in the region of overlap. The comparison with neutrino data from CDHS on F_2, to which the factor 5/18 predicted by QPM has been applied, also works well.

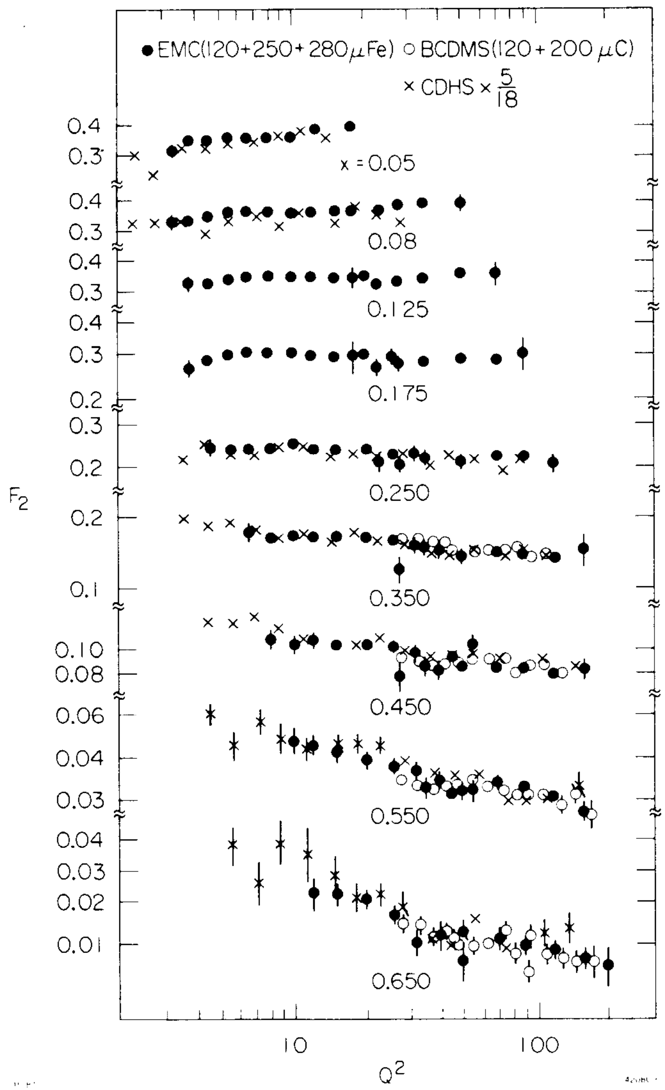

Fig. 3. $F_2(x, Q^2)$ measured by EMC (●), BCDMS (O) with μ and by CDHS with ν, $\bar{\nu}$ (x).

Figure 4 shows $xF_3(x, Q^2)$ as measured by CDHS[6] and Gargamelle.[9]

Both $F_2(x, Q^2)$ and $xF_3(x, Q^2)$ show a Q^2 dependence which is different at different values of x, as observed for the first time in a muon experiment in 1973.[20]

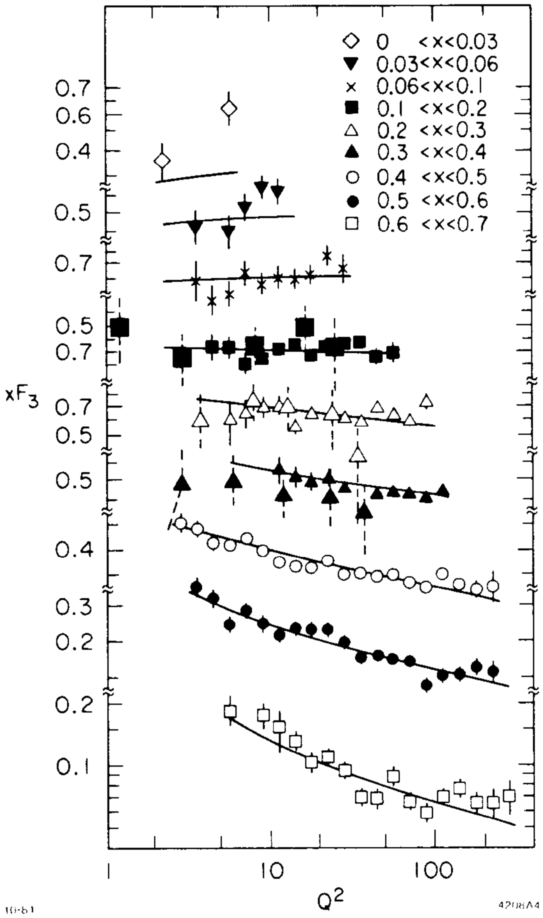

Fig. 4. xF_3 measured by CDHS. The points with broken error bars are from the GGM experiment.

Sources of Scaling Deviation

There may be several sources of Q^2 dependence.

1. There are purely kinematic effects such as non zero mass target. It can be demonstrated that this induces a $1/Q^2$ scaling violating term, which can be taken into account by a change of variable

$$x \to \xi = \frac{2x}{1 + \left(1 + \frac{4m^2x^2}{Q^2}\right)^{1/2}} .$$

These effects are important only at low Q^2.

2. There is a threshold effect for the production of heavy flavors. This also is a purely kinematic effect related to the heavy mass of the produced particles. This effect can be a significant source of scaling violation (~30%) at low x in μ data, and it can be measured in multi-muon experiments.[3,21]

3. There are all those dynamical effects which reflect coherent phenomena such as scattering on multiquark structures, or quark transverse momentum, or resonance production that induce a $1/Q^n$ dependence and go under the name of higher twist terms from the language of the operator product expansion.

4. Gluon emission, which is treated by conventional QCD and governed by the probability of radiation

$$\alpha_S = \frac{4\pi}{\frac{33 - 2n_f}{3} \ln Q^2/\Lambda^2}$$

which every experiment tries to measure.

"Conventional QCD" Analysis

If one wants to analyze the data in terms of the gluon radiation hypothesis, there is an almost standard method to follow: it consists of starting with the Altarelli-Parisi equation[22] which gives the Q^2 evolution in QCD for all the structure functions. The non-singlet case (i.e., xF_3, $F_2^p - F_2^n$, or F_2 for $x > 0.4$) is favored because its evolution is not coupled to the gluon distribution $G(x, Q^2)$. On the other hand, the Q^2 evolution of the singlet case allows one to determine $G(x, Q^2)$ if Λ is known.

The second step is to solve (in leading order or next to leading order) the A-P equation, assuming a parameterization of F_i of the kind $F_i = Ax^\alpha(1-x)^\beta(1+\gamma x)$ and finally determine all the parameters involved in the fit, namely A, α, β, γ, and Λ. A summary of recent results is given in Table III. Note that the range of Q^2 is different for different fits. Changes in R from R = 0 to R = .2 cause a large decrease in the value of Λ. Including non-leading order QCD terms in the analysis in some cases increases Λ and in other cases decreases Λ, depending on how the analysis is done. It is not very meaningful to compare the different Λ values, for there are quite strong variations due to the calculation used or to the assumed value of R. If one combines the results on $\Lambda_{\overline{MS}}$ from CDHS, BEBC, EMC, and BCDMS experiments to obtain a value for α_S, one gets

$$\alpha_S^{\overline{MS}}\ (100\ \mathrm{GeV}^2) = .146^{+.051}_{-.034}\ , \text{ if } n_f = 4 \quad . \qquad (5)$$

Shown in Fig. 5 are the high statistics EMC μ data along with their QCD fit.

Higher Twist

A hadron is never just an isolated quark so a complete treatment of deep inelastic scattering must include both gluonic radiation and hadron structure effects. Attempts to do this in the framework of QCD have been carried on by several theorists, both in a general treatment of power corrections on the basis of the operator product expansion,[25] and in a more phenomenological way predicting some specific experimental consequences.[26] The important thing to do experimentally is to isolate and measure the strength of the higher twist terms. These

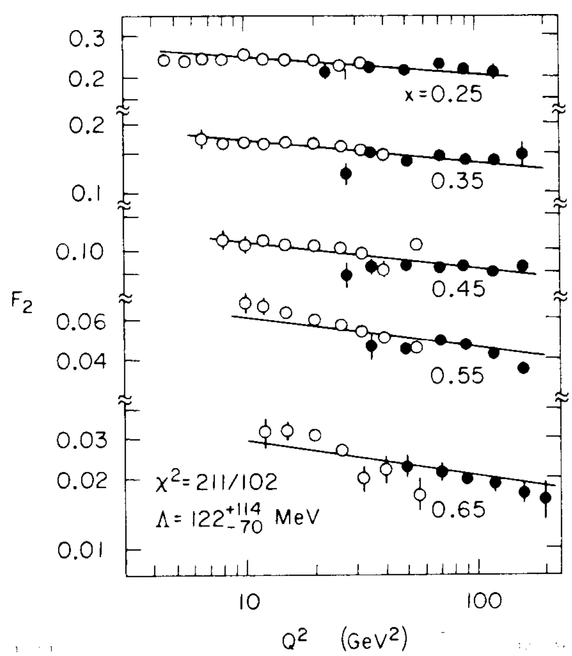

Fig. 5. QCD fit to μ-Fe data of the EMC collaboration.

Table III. Results on Λ from different experiments. The B.G. method is described in Ref. 23 and G.A.L.Y. method in Ref. 24.

Expt	Data Used (Q^2 in GeV^2)	Method	Λ (MeV)
CDHS Iron, WB + NB	xF_3 and F_2 for $x > .4$ $Q^2 > 2.$	A.-P. R = .1 $(Q^2 > 10)$	 $90 < \Lambda_{\overline{MS}} < 300$ (140 ± 60)
CHARM	xF_3, F_2 $Q^2 > 3.$	B.-G. R = 0.	$290\ ^{+120}_{-120}\ ^{+100}_{-100}$
GGM C_3H_8, WBB	xF_3 and F_2 for $x > .4$ $Q^2 > 2.$	A.-P. R = .1	 $20\ ^{+90}_{-20}$
BEBC Ne - H	xF_3 for $x < .4$ F_2 for $x > .4$ $Q^2 > 2.$	G.A.L.Y.	$\Lambda_{\overline{MS}} = 140\ ^{+95}_{-35}$
BCDMS Carbon $E_\mu = 120, 200$	$NS \equiv F_2$ for $.3 < x < .7$ $Q^2 > 20.$	A.-P. R = 0	 $85\ ^{+60}_{-40}\ ^{+90}_{-70}$
		NLO	$85\ ^{+53}_{-40}\ ^{+80}_{-67}$
		B.G.	$136\ ^{+50}_{-40}\ ^{+90}_{-80}$
EMC Hydrogen $E_\mu = 120, 280$	F_2 for $x > .25$ $Q^2 > 7.$	A.-P. R = 0	 $110\ ^{+160}_{-80}$
		R = .2	$37\ ^{+36}_{-22}\ ^{+84}_{-30}$
		NLO	$170\ ^{+135}_{-105}$
Iron $E_\mu = 250, 280$	F_2 for $x > .25$ $Q^2 > 4.5$	A.-P. R = 0	 $122\ ^{+120}_{-70}$
		R = .2	$41\ ^{+12}_{-19}\ ^{+86}_{-32}$
		NLO	$145\ ^{+150}_{-90}$

have a dependence on kinematic variables different from that of the asymptotically dominant twist 2 term. They can be a very small part of the total cross section, so their effects must be searched for in those restricted regions of space phase ($x \to 1$ or large p_T) where they could dominate, or in some observables and special processes (Drell Yan, semi-inclusive π production by leptons). For example, $R = \sigma_L/\sigma_T$ is a good observable because gluon radiation effects are expected to be different ($R \neq 0$ at low x) from those due to higher twist (diquark model[27] predicts $R \neq 0$ at high x) (Fig. 6).

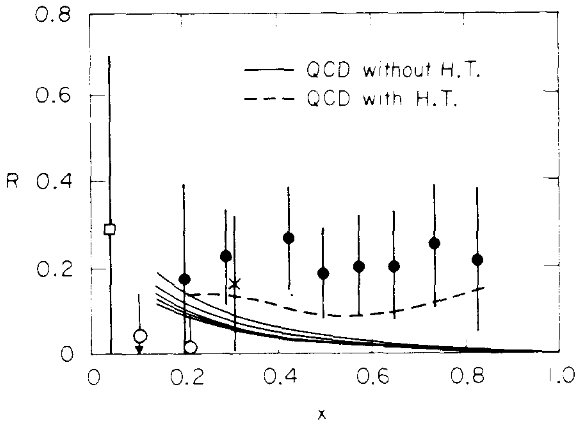

Fig. 6. SLAC-MIT data on R. The curves are from Ref. 27.

There exist some precise predictions for semi-inclusive π production in deep inelastic scattering.[28] For example, in $\nu N \to \mu^- \pi^+ X$ a special kind of higher twist process predicts an extra $(1-y)$ component to the flat y distribution ($z = E_\pi/\nu$):

$$\sigma(y, Q^2, z) \,\alpha\, (1 - z)^2 + \frac{4}{9} \frac{\langle k_T^2 \rangle}{Q^2} (1 - y) \qquad (6)$$

Looking at the y distribution for $z \to 1$ ($z > .5$), the Gargamelle ν collaboration[29] measured a strength for the high twist contribution of $\langle k_T^2 \rangle \sim 1\ \text{GeV}^2$. Note that this scale of 1 GeV is large with respect to Λ. Even if it is not obvious how to go from a semi-inclusive process to inclusive lepto production, the Gargamelle information suggests that above $Q^2 = 10\ \text{GeV}^2$ higher twist effects alone cannot be responsible for scaling violation.

In inclusive lepto production there is no prediction for the size of higher twist effects. The data available now at high Q^2 and in an x region safe from their contributions show that Λ is smaller than that determined in lower Q^2 region, suggesting that for $Q^2 < 10\text{-}15\ \text{GeV}^2$ power corrections are important.

Usually a parameterization of the type:

$$F_i(x, Q^2) = F_i^{QCD}(x, Q^2) \left[1 + f(x) \frac{M^2}{Q^2} + f(x) \frac{M^4}{Q^4} \; \ldots \right] \qquad (7)$$

is assumed. This means that higher twist can significantly change the value of Λ, because Λ and M^2 are completely correlated in the fit to data.

Muon experiments have data in (x, Q^2) region, $Q^2 > 20\ \text{GeV}^2$, $x < .6$ where they can be considered safe from higher twist contributions.

An attempt was made by M. Leenen of the EMC collaboration[18] to combine EMC μp data with SLAC ep data. With the parameterization

$$F_2(x, Q^2) = F_2^{QCD}(x, Q^2)\left(1 + \frac{f(x)}{Q^2}\right) \quad ,$$

a fit to each bin of x was done to obtain the shape f(x). The result is $\Lambda_{\overline{MS}} = 122^{+66}_{-51}$ MeV, and $f(x) = x^2/(1 - x)^2$. The higher twist contributions are important only for $x > .5$.

Similar information was obtained by F. Eisele[30] also using SLAC data but with a slightly different method. A value of Λ determined in the high W^2 region by CDHS data was used to extrapolate a QCD curve to the low Q^2 region of the SLAC ed data on F_2. Without a higher twist contribution, the QCD curve with $\Lambda = .2$ GeV does not go through the SLAC points (Fig. 7). From a fit to $F_2 = F_2^{QCD} + F_2^{H.T.}$ the conclusion was that a shape $F_2^{H.T.} = x^2(1 - x)/Q^4$ or $F_2^{H.T.} = x^2(1 - x)/Q^2$ is in good agreement with SLAC data, which is the same conclusion as from EMC analysis. This shape is consistent with that expected from the diquark model of Ref. 27. The high twist scale found was $M^2 =$ $1.5 \pm .2$ GeV^2, again large compared to Λ.

Conclusions

1. Data from high energy μ, ν experiments on structure functions are in good agreement and their Q^2 dependence is described by $\Lambda \approx 100$ MeV.
2. It will be very difficult to significantly improve such a set of data in the near future.
3. Better precision on F_2 requires measurement of R.
4. Higher order corrections $O(\alpha_s^2)$ hardly affect the quality of the fits.
5. Higher twist terms are present for $x > .5$ and $Q^2 < 15$ GeV^2.

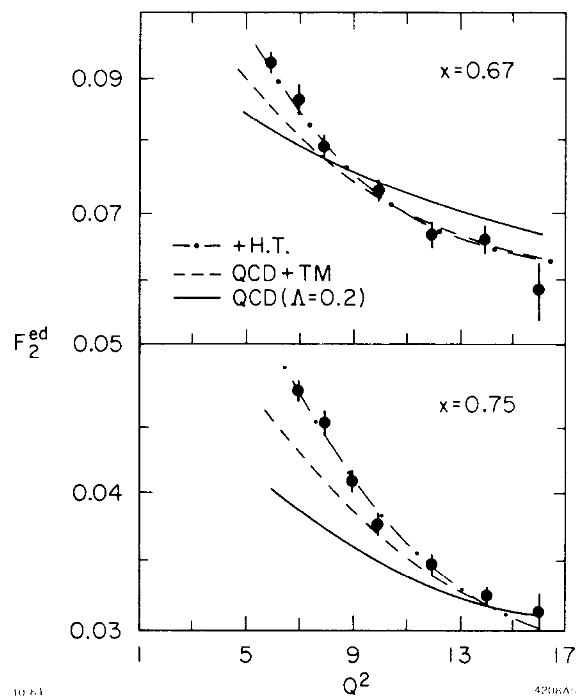

Fig. 7. Comparison between QCD curve calculated with Λ = .2 determined by CDHS at high W^2 and SLAC data in small Q^2 region and fixed x.

Is QCD now tested through scaling violations? There is an intrinsic difficulty for clean tests of QCD in the non-scaling behavior of structure functions, because the effect to be measured is small at large Q^2. If Λ is small the systematic errors become extremely important. On the other hand, where α_S is larger, that is at smaller Q^2, higher twist terms complicate the situation and must be included properly before gluon radiation effects are really tested.

Nevertheless, QCD accounts qualitatively for a large range of data. Much experimental information taken together should finally prove that α_S decreases logarithmically with Q^2.

REFERENCES

1. Bologna-CERN-Dubna-Munich-Saclay collaboration, CERN-EP/81-58.

2. European Muon collaboration, CERN-EP/81-84.

3. G. D. Gollin et al., Phys. Rev. D24, 559 (1981).

4. M. Strovink talk at this conference.

5. M. Tenner (Amsterdam, Bologna, Padova, Pisa, Saclay, Torino collaboration). Proceedings of Conference on ν Physics and Astrophysics, Hawaii, July 1981.

6. J.G.H. De Groot (CERN-Dortmund-Heidelberg-Saclay collaboration). Proceedings of XX Conference on HEP, ed. by L. Durand and L. Pondrom, Madison 1980, p. 735.

7. Cal. Tech., FNAL, Rochester, Rockefeller collaboration. Proceedings of Madison Conference 1980, p. 741.

8. Charm collaboration. CERN-EP.

9. J. Morfin et al., Phys. Lett. 104B, 235 (1981).

10. P. Musset, J. P. Vialle, Phys. Rep. 39C, 3 (1978).

11. P. Bosetti et al., Nucl. Phys. B142, 1 (1978).

12. D. Sinclair, Proceedings of Bergen ν Conference 1979, p. 343.

13. A. Benvenuti et al., Phys. Rev. Lett. 42, 1317 (1979).

14. E. M. Riordan et al., SLAC-PUB 1634 (1975).

15. M. D. Mestayer, SLAC-Report 214 (1978).

16. H. L. Anderson et al., Phys. Rev. Lett. 38, 1450 (1977).

17. B. A. Gordon et al., Phys. Rev. D20, 2645 (1979).

18. Talk by J. Drees, Bonn Conference 1981.

19. J. Knobloch (CDHS collaboration). Proceedings of XX Conference on HEP, ed. by L. Durand and L. Pondrom, p. 769.

20. D. J. Fox et al., Phys. Rev. Lett. 33, 1504 (1974). Y. Watanabe et al., Phys. Rev. Lett. 35, 898 (1975).

21. J. J. Aubert et al., XX International Conference on HEP, Wisconsin 1980, p. 205.

22. G. Altarelli, G. Parisi, Nucl. Phys. B126, 298 (1977).

23. A. J. Buras, K.J.F. Gaemers, Nucl. Phys. B132, 249 (1978).

24. A. Gonzales-Arrojo et al., Nucl. Phys. B153, 161 (1979). Nucl. Phys. B166, 429 (1980).

25. H. D. Politzer, Nucl. Phys. B172, 349 (1980). R. L. Jaffe, M. Soldate, CTP 937, June 1981. M. A. Shifman et al., Nucl. Phys. B147, 385 (1979), and references therein.

26. E. L. Berger, S. Brodsky, Phys. Rev. Lett. 42, 940 (1979). E. L. Berger, S. Brodsky, SLAC-PUB 2749.

27. L. F. Abbott, E. L. Berger, R. Blankenbecler and G. L. Kane, Phys. Lett. 88B, 157 (1979). L. F. Abbott, W. B. Atwood and R. M. Barnett, Phys. Rev. D22, 582 (1980).

28. E. L. Berger, Phys. Lett. 89B, 241 (1980). E. L. Berger, Zeit. Phys. C4, 287 (1980).

29. M. Hagnenauer et al., Phys. Lett. 100B, 185 (1981).

30. F. Eisele. DO-EXP 6/81.